JOURNAL GEOLOGICAL SOCIETY OF INDIA
Vol.81, March 2013, pp.369-376

# Geology, Petrography and Geochemistry of Rhyolite-Hosted Uranium Mineralization at Mohar, Shivpuri District, Madhya Pradesh

Shailendra Kumar[1*], Madhupurna Roy[1], Pradeep Pandey[1],
C. L. Bhairam[1] and P. S. Parihar[2]
Atomic Minerals Directorate for Exploration and Research, Department of Atomic Energy,
Government of India, [1]New Delhi - 110 066; [2]Hyderabad - 500 016
*Email: shail_kin64@yahoo.co.uk

**Abstract:** In the westernmost part of the Bundelkhand Granitoid Complex (BGC), a mesa structure represents a unique outlier, surrounded by brecciated granite and filled with Vindhyan sedimentary rocks locally known as the Dhala Formation near Mohar village of Shivpuri district, Madhya Pradesh. Uranium mineralisation located in the area is mostly associated with rhyolite of peralkaline to peraluminous in nature, that has a high average uranium concentration (30 ppm). The mineralization is in or adjacent to caldera and is hydrothermal vein-type. Radioactivity is mainly due to coffinite with limited radioactivity due to U-Ti complex, uranium adsorbed in clay and labile uranium along fracture. Coffinite occurs in association with pyrite and chalcopyrite or chlorite with presence of fluorite. Features such as chloritisation, clay formation and sulfide mineralisation manifest hydrothermal alteration. Chemical analysis indicates the aluminous nature of the rock and their high $K_2O$ / $Na_2O$ (3.81-12.84) ratios are suggestive of predominance of potash feldspar over sodic. The alteration index varies from 49.88-92.40, which, reflects high intensity of hydrothermal alteration. Chlorite-carbonate-pyrite index (CCPI), a measure of the intensity of replacement of sodic feldspars and glass by sericite, chlorite, carbonate, and pyrite associated with hydrothermal alteration proximal to the ore bodies varies from 3.84-49.66.On the basis of core study, geochemistry and mineralogy, it is envisaged that epigenetic hydrothermal solutions were responsible for concentration of uranium as coffinite, radioactive carbonaceous matter and adsorbed uranium phases in rhyolite with sulfide confined to weak planes.

**Keywords:** Bundelkhand Granitoid Complex (BGC), Geochemistry, Hydrothermal uranium mineralisation, Madhya Pradesh.

## INTRODUCTION

The Mohar (25°17'59.7": 78° 08'3.1"; 54K/3) calderon forming a flat-topped hill is situated in the westernmost part of Bundelkhand craton about 50 km SW of Jhansi in the Shivpuri district of Madhya Pradesh. It is 7.5 km in diameter with intra-cauldron sedimentary rocks representing the Dhala Formation, equivalent to the Semri Group of the Vindhyan Supergroup in the centre, unconformably overlain by purple sandstone equivalent to the Sumen sandstone of the Kaimur Group. This structure associated with felsic volcanic rocks was conceptualised by Jain et al. (2001) as a cauldron. The origin of the Mohar structure is still debatable, as in the opinion of Jain et al. (2001), it is formed as a result of central Plinian-type volcanic explosion, whereas, Pati and Reimold (2007) and Pati et al. (2008) view it as an impact-related structure.

Felsic volcanic rocks have long been considered as a primary source of uranium for major uranium deposits (Nash, 2010) and deposits in rhyolitic rock are known world-wide (Castor et al., 2000). The Atomic Minerals Directorate for Exploration and Research (AMD) is carrying out geological investigations including drilling in the Mohar area for the possibility of locating uranium mineralization in and adjacent to the Mohar structure. Significant, uranium mineralization hosted by rhyolite is intercepted in a few boreholes drilled in the area. Understanding the geology, mineralogy, geochemistry and possible genesis of these deposits is worthwhile, to help present and future exploration in similar types of terrain. This paper characterizes the geology, mineral assemblage and chemistry of the uranium mineralization and discusses its possible origin.

## GEOLOGICAL SETTING

The Bundelkhand Massif comprises mainly granitoids of different episodes, low to high grade metamorphites of

0016-7622/2013-81-3-369/$ 1.00 © GEOL. SOC. INDIA

pelitic, psammatic, mafic and ultramafic rocks, quartz_reefs and mafic dyke swarms. The Bundelkhand Granitoids exposed all through the Massif have been divided into five types of granites, viz., hornblende granite, biotite granite, coarse-grained porphyritic granite and two phases of younger pink and fine-grained leucogranite, by several workers (Rahman and Zainuddin, 1993; Sharma and Rahman, 1998). The detailed account of rock types and their interrelationship has been discussed by Basu (1986).

The area around Mohar exposes rocks of the Neo-Archaean to Paleo-Proterozoic Bundelkhand Gneissic Complex (BGC), unconformably overlain by the sedimentary rocks of Meso-Neo Proterozoic Vindhyan Supergroup. Three types of granites, namely, hornblende granite, fine-grained leucocratic granite and fine-grained pink biotite granite, besides volcanic rocks like rhyolite, occur in the area. The Mohar structure having 7.5 km-diameter is defined by an oblate central part surrounded by outcrops of brecciated granite. The central 4.5 km-diameter comprises flat-lying Sumen sandstone Formation of Kaimur Group succeeded by argillaceous/arenaceous sedimentary rocks of the Vindhyan Supergroup displaying cyclic sedimentation with lateral as well as vertical facies. The Dhala sandstone is mainly of two types, viz., a poorly compacted arkosic variant and a well compacted gritty variety. These sedimentary rocks show 3°-5° centripetal dip. Penecontemporaneous deformation structures like graded, convolute and contorted bedding are present. The Dhala sedimentary rock has remained unaffected by deformations and hydrothermal alteration suggesting a pre-Dhala tectonic activity. Underlying the Dhala sedimentary rocks with a distinct unconformity are felsic volcanic rocks represented by pink to brick red, vesicular to non-vesicular rhyolite and tuffs with distinct flow structures, scantly exposed as isolated small outcrops in the well cuttings in the paddy fields. Drilling data, however, revealed the occurrence of continuous sheet-like body below the sedimentary rocks having thickness upto 200 m in the central part of the Mohar structure. The area surrounding Mohar is demarcated by intense brecciation of granitoids. The effect of tectono-magmatic activity in the area during the post–collapse period is evidenced by the presence of

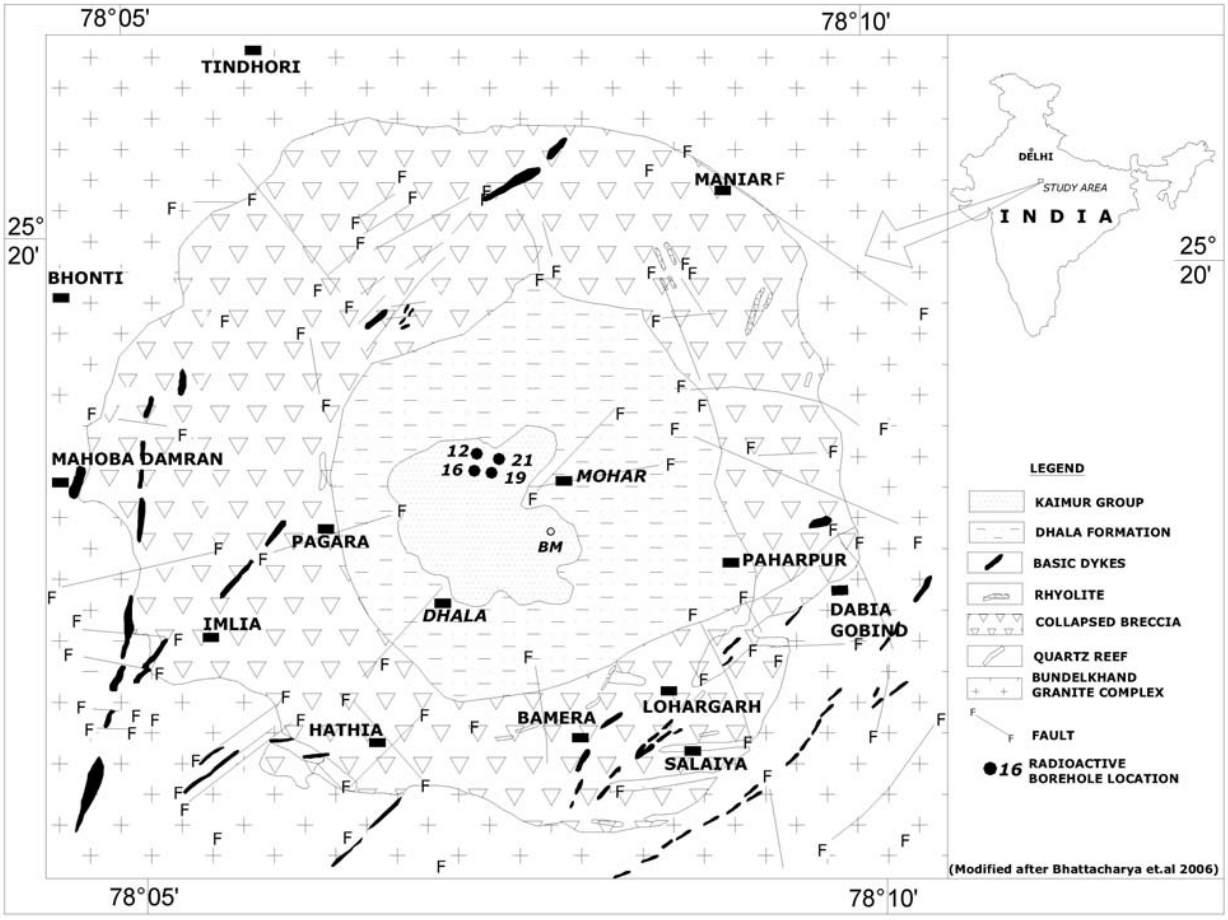


**Fig.1.** Geological map of the Mohar area showing borehole locations.

younger granite and pink rhyolite (Bhattacharya and Rao, 2006). Several NE-SW trending quartz reefs transect the igneous rocks of the area implying emplacement at a very late-stage of crustal evolution in Bundhelkhand. NW-SE trending basic dykes constitute the youngest phase of magmatism in the area as suggested by their field relationship. The rocks of the area have been affected by a prominent NE-SW and NW-SE trending faults/ fractures with extensive mylonitisation and S-C plane development at meso- and microscopic scales. The joints overall display a radial trend, although they are slightly accentuated along E-W, NNE-SSW and NW-SE directions (Fig.1).

## URANIUM MINERALIZATION

Drilling carried out from the top of the Mohar structure brought to light uranium mineralization in borehole MCB-12 hosted by rhyolite below the cover of the Vindhyan sedimentary rocks. Significant mineralization was also intercepted in boreholes MCB-16, MCB-19 and in MCB-21 establishing persistency over a stretch of 200 m in a NE-SW direction (Fig.2). Mineralized boreholes are localized and confined to the northeastern part of the Mohar structure.

Detailed lithological study of the borehole cores reveal that mineralization is essentially hosted by pink to brick red, fine-grained, vesicular to non-vesicular rhyolite and tuffs with distinct flow structures and closely associated with the fractures and weak planes with ample evidences of hydrothermal alterations. The rock fragments in tuff are of variable size <1 mm to >5 cm and sub-angular to angular consisting of quartz, feldspar and granite fragments. The vesicles in rhyolite are filled with colloidal silica, clay, carbonaceous material and chlorite. Veins filled by secondary silica are abundant. Fracture-filling is in the form of clay, chlorite, goethite, hematite, carbonaceous matter and sulfides. The associated minerals present are chalcopyrite, pyrite, galena and molybdenite as fracture-filling in veins and dissemination. Hydrothermal alteration such as silicification, chloritisation, sericitisation, ferruginisation and kaolinisation are noticed.

Borehole MCB-16 in, which, radioactivity continues upto 452.15 m depth, with rhyolite and tuff having thickness of 206 m (Fig.3) was selected for detailed study. Rhyolite samples from different depth were collected to fully examine and compare radiometric data, lithology, chemical data and

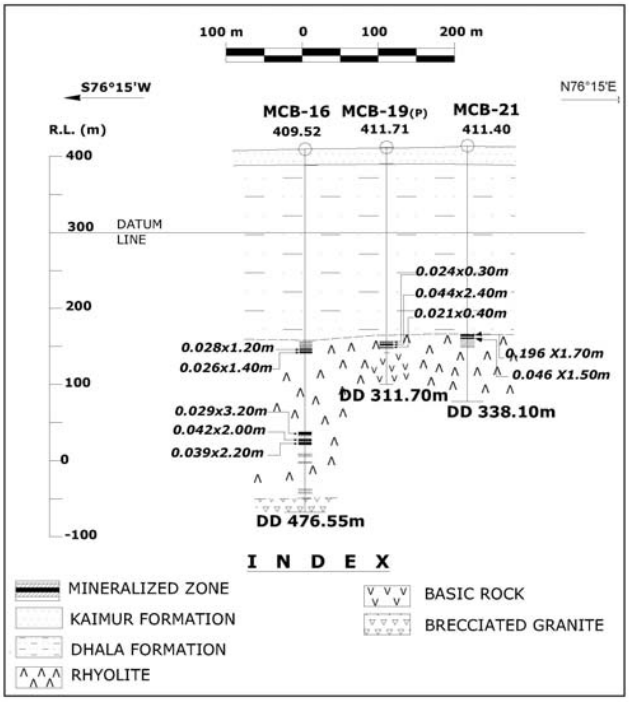


**Fig.2.** NE-SW geological section through borehole nos. MCB-16, 19 and 21.

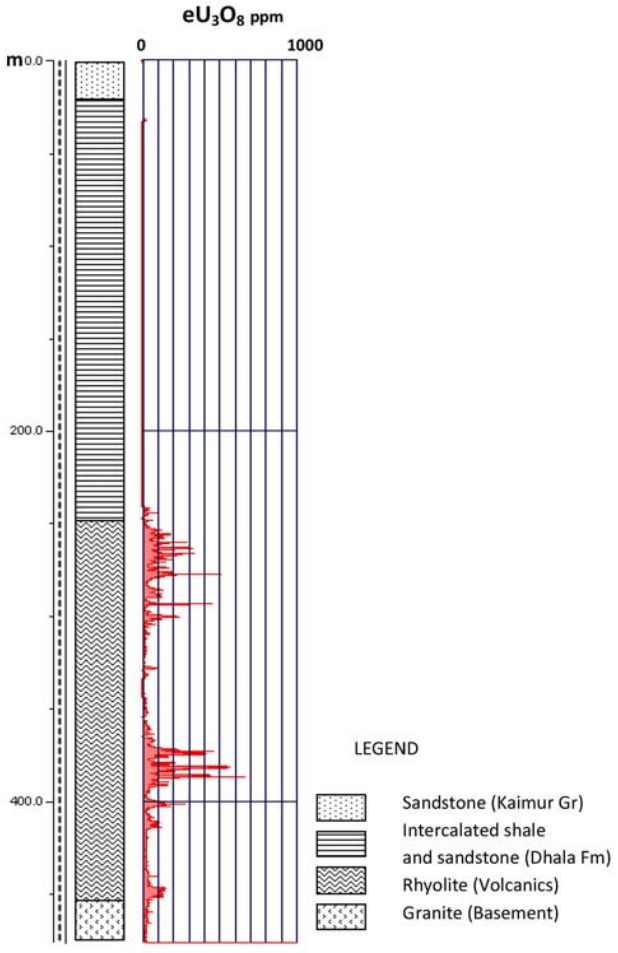


**Fig.3.** Litholog and gamma ray logging results of borehole MCB-16

petrological information to understand the possible controlling factors for uranium mineralization in Mohar.

## PETROGRAPHY OF RADIOACTIVE ROCKS

The host for uranium mineralization is identified as rhyolite/rhyolite tuff characterized by red to buff-coloured, glassy to micro-crystalline felsic groundmass with shapeless patches of cristobalite and clasts of quartz, feldspar, granite and basic rock embedded in varying proportions. The rock is groundmass-dominated at places and clasts-dominated at others. It is often fractured and affected by later hydro-thermal solution activity resulting in silicification, chloritisation and sulfide formation, with secondary quartz and an assemblage of pyrite, chalcopyrite, galena and sphalerite, distributed along veins and fractures of the rock. Radioactivity is chiefly due to coffinite with subordinate amounts of U-Ti complex, uranium adsorbed in clay and labile uranium along fracture. Pyrite, chalcopyrite and chlorite are commonly associated with uranium. The U-Ti complex occurs in association with rutile along weak planes. Coffinite varies from opaque to translucent olive green to brown, with ill-defined outline and isotropic nature (Fig.4). It is marked by high radioactivity manifested by highly dense alpha tracks after 5 days of exposure to LR-115 film and also by positive chromogram. It occurs as disseminations at grain niches and boundaries and as veins and fracture fills, invariably associated with pyrite and chalcopyrite or chlorite. The U-Ti complex is waxy brown, translucent, marked by medium density alpha tracks, negative chromogram and in association with rutile distributed along weak planes.

Hydrothermal alteration induced by solution activity is recorded along post-consolidation fractures in litho-types below the unconformity. This is manifested as secondary infiltration of quartz, carbonate, chlorite, clay, pyrite-chalcopyrite-galena-sphalerite and radioactive minerals viz. coffinite with subordinate amounts of U-Ti complex, uranium adsorbed in clay and labile uranium. Fluorite is noted in association with quartz (Fig.5). It is observed that most of the radioactive phases are confined to fractures that cross cut the flow direction of the melt, wherever, it is discernible. This reiterates the role of tectonics and hydrothermal processes being instrumental in bringing about mineralization. Sulfides and chlorite indicate possible reducing environment prevailing during precipitation of the uranium minerals. The presence of these, together with fluorite, indicates hydrothermal solution activity. The non-radioactive samples representing zones of similar lithology show lesser fracturing and consequently lower hydro-thermal activity, and hence, lack of mineralization.

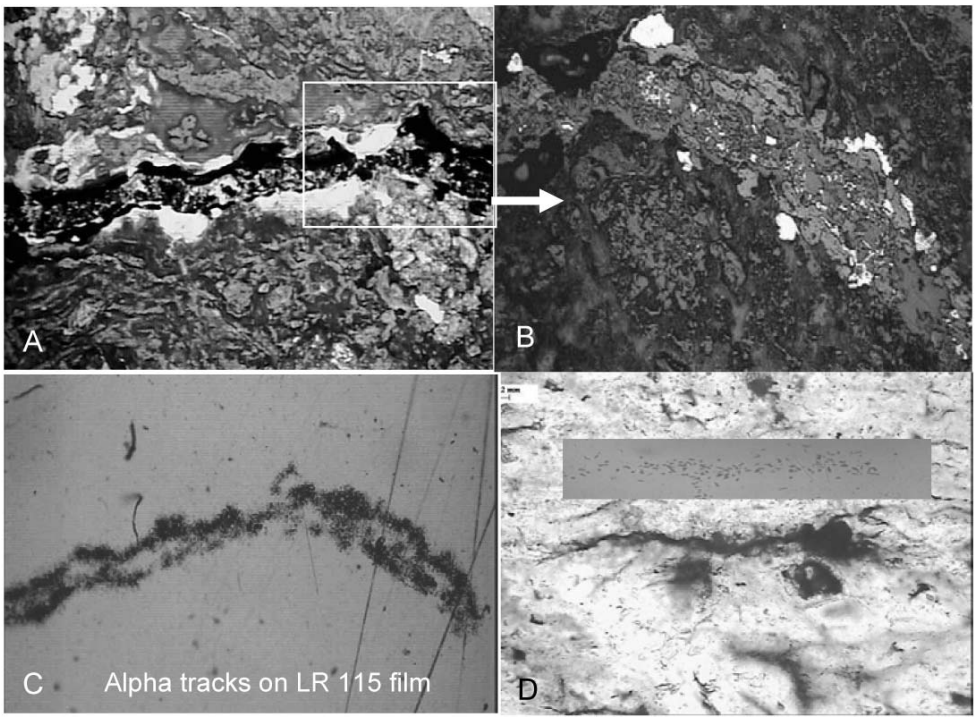


**Fig.4.** Hydrothermal coffinite in rhyolite MCB-16/373.90. A, C in transmitted light, 1N; B in relfected light, IN. D Labile uranium along fracture plane MCB 16/288.62 with corresponding alpha tracks on LR 115 film placed above.

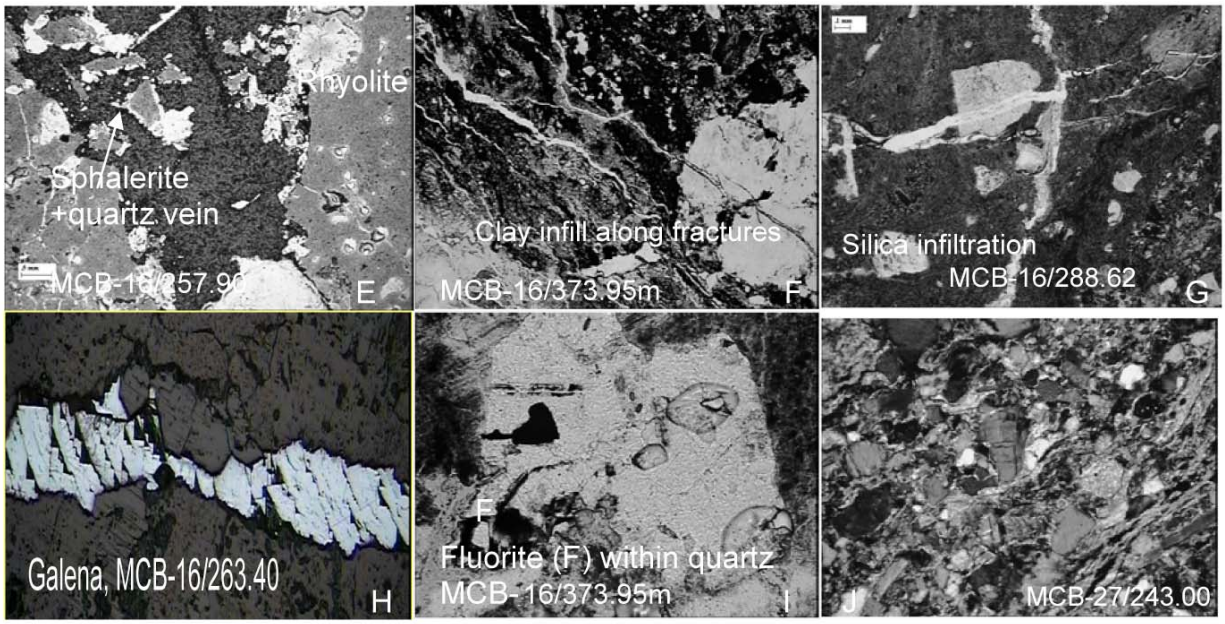


**Fig.5.** Photomicrographs depicting hydrothermal alteration in transmitted light. E to I under 1N; J under XN.

## GEOCHEMISTRY

### Major and Trace Elements

Twelve representative radioactive and non-radioactive core samples from borehole MCB-16 of rhyolite (n = 12) were analysed for uranium, major and minor oxides (wt. %) and trace element content (Table 1). Evaluation of data shows that the rhyolite displays a wide range of variations in major oxides such as $SiO_2$ 61.1-75.1wt. %, $Al_2O_3$ 9.13-13.15 wt. %, $Fe_2O_3$ 1.29- 4.63wt.%, FeO 0.43 - 3.13 wt.%, MgO 0.38 - 4.16 wt.%, CaO 0.1 - 4.33 wt.%, $Na_2O$ 0.73 -1.58wt.% and $K_2O$ 6.02-10.54 wt.%, which suggest high degree of fractional crystallization. The $K_2O$ and MgO contents are generally higher, with the $Na_2O$ content much lower than the average rhyolite. An admixture of both felsic (potassic) and mafic (chloritic) material in the rhyolite groundmass may have resulted in varying amounts of $K_2O$, MgO and FeO. The $K_2O$ / $Na_2O$ ratio varies from 3.81 to 12.84 due to the enrichment of potash feldspar over sodic and possibly due to alteration. Total alkalis vary from 7.39 to 11.49 %. The rhyolite is mostly peralkaline to peraluminous, with the A/CNK ratio varying from 0.43 to 1.42. The felsic index ranges from 56.26 to 99.14. The alteration index (AI= 100 (MgO+$K_2O$) / (MgO+$K_2O$+$Na_2O$+CaO), varies from 49.88 to 92.40, which, reflects medium to high intensity of hydrothermal alteration for the samples. The index varies from values of 20 to about 60 for the unaltered rocks, and between 50 and 100 for the hydrothermally altered rocks; with AI tending towards 100 as the alteration reaches maximum intensity (Ross R Large et al. 2001). As the alteration intensity progresses, the $K_2O$ and MgO amounts increase, with a concomitant decrease in $Na_2O$ and CaO. The chlorite-carbonate-pyrite index (CCPI = 100 (MgO+FeO) / (MgO+FeO+$K_2O$+$Na_2O$), a measure of the intensity of replacement of sodic feldspars and glass by sericite, chlorite, carbonate, and pyrite, associated with hydrothermal alteration proximal to the ore bodies, has low values that vary from 3.84 to 49.66.The CCPI index is useful to trace the role of the more common alteration minerals, chlorite, Fe-Mg carbonates and pyrite, typically developed in the inner alteration zone of many ore deposits. Low values of CCPI index for the borehole core samples of the area reflects low intensity of chlorite, pyrite and Fe-Mg carbonate replacement.

Trace element contents indicate higher value of Cu (480 ppm) and Co (45 ppm) for the radioactive samples (n = 8) as compared to Cu (29 ppm) and Co (23 ppm) for the non- radioactive samples (n = 4) implying enrichment of these elements with uranium in hydrothermal solutions. Cr values are high as compared to the average rhyolite. Ni does not show any distinct trend in radioactive and non-radioactive samples. High Pb values are observed in the non-radioactive and radioactive samples, and some highly radioactive samples have low Pb values, probably due to non- radiogenic lead, galena, having been reported from the area. The uranium chemical data indicated that an average 85% of the contained uranium could be extracted by conventional leaching.

**Table 1.** Major, minor (in wt %) and trace element (in ppm) data for the Mohar rhyolite

| | MC1 | MC2 | MC3 | MC4 | MC5 | MC6 | MC7 | MC8 | MC9 | MC10 | MC11 | MC12 | MAX | MIN |
|---|---|---|---|---|---|---|---|---|---|---|---|---|---|---|
| $SiO_2$ | 67.2 | 75.1 | 67.4 | 72.3 | 67.8 | 71.87 | 64.31 | 61.1 | 59.91 | 67.56 | 67.91 | 71.9 | 75.1 | 59.91 |
| $TiO_2$ | 0.25 | 0.45 | 0.46 | 0.38 | 0.3 | 0.31 | 0.52 | 0.82 | 0.21 | 0.39 | 0.43 | 0.34 | 0.82 | 0.21 |
| $Al_2O_3$ | 11.2 | 9.13 | 12.23 | 9.73 | 13.15 | 12.59 | 12.93 | 13.04 | 10.42 | 12.93 | 12.37 | 11.24 | 13.15 | 9.13 |
| $Fe_2O_3$ | 1.37 | 1.47 | 1.76 | 1.51 | 1.29 | 1.81 | 3.87 | 4.63 | 0.34 | 1.72 | 1.96 | 1.3 | 4.63 | 0.34 |
| FeO | 0.43 | 0.83 | 1.4 | 0.93 | 0.72 | 0.68 | 2.08 | 3.13 | 0.22 | 1.47 | 1.51 | 1.15 | 3.13 | 0.22 |
| MnO | 0.1 | 0.02 | 0.03 | 0.02 | 0.02 | 0.02 | 0.09 | 0.12 | 0.18 | 0.03 | 0.03 | 0.03 | 0.18 | 0.02 |
| MgO | 0.38 | 1.25 | 2.23 | 1.2 | 1.07 | 0.85 | 3.2 | 4.16 | 0.16 | 2.28 | 2.07 | 1.5 | 4.16 | 0.16 |
| CaO | 4.33 | 0.24 | 0.25 | 0.14 | 0.1 | 0.6 | 0.18 | 0.28 | 7.4 | 0.26 | 0.15 | 0.15 | 7.4 | 0.1 |
| $Na_2O$ | 0.84 | 1.58 | 1.16 | 0.73 | 0.95 | 1.26 | 1.26 | 1.37 | 1.16 | 1.37 | 1.58 | 1.16 | 1.58 | 0.73 |
| $K_2O$ | 9.88 | 6.02 | 8.5 | 9.37 | 10.54 | 8.87 | 6.52 | 6.02 | 8.36 | 7.36 | 6.86 | 7.02 | 10.54 | 6.02 |
| $P_2O_5$ | 0.77 | 0.63 | 0.77 | 0.73 | 0.77 | 0.72 | 0.82 | 0.79 | 1.03 | 0.82 | 0.95 | 0.76 | 1.03 | 0.63 |
| LOI | 0.87 | 1.54 | 1.94 | 1.2 | 1.15 | 0.98 | 2.65 | 3.24 | 9.24 | 2.03 | 1.81 | 1.47 | 9.24 | 0.87 |
| $U_3O_8$(T) | 0.033 | 0.063 | 0.053 | 0.097 | 0.033 | 0.11 | 0.099 | 0.105 | 0.004 | 0.004 | 0.005 | 0.012 | 0.11 | 0.004 |
| **Total** | **97.65** | **98.32** | **98.18** | **98.34** | **97.89** | **100.67** | **98.53** | **98.81** | **98.63** | **98.22** | **97.63** | **98.03** | **100.67** | **97.63** |
| Cr | 80 | 76 | 48 | 80 | 60 | 80 | 80 | 80 | 40 | 60 | 72 | 80 | 80 | 40 |
| Ni | 23 | 16 | 18 | 23 | <10 | <10 | <10 | 20 | <10 | 96 | <10 | <10 | 96 | 16 |
| Co | 54 | 33 | 30 | 61 | 39 | 39 | 45 | 56 | 28 | 21 | 18 | 25 | 61 | 18 |
| Cu | 44 | 518 | 90 | 478 | 80 | 2056 | <5 | <5 | 99 | 8 | <5 | <5 | 2056 | 8 |
| Pb | 2080 | 3570 | 173 | 6990 | <10 | <10 | 82 | 136 | 1500 | 245 | <10 | 3570 | 6990 | 82 |
| $K_2O/Na_2O$ | 11.76 | 3.81 | 7.33 | 12.84 | 11.09 | 7.04 | 5.17 | 4.39 | 7.21 | 5.37 | 4.34 | 6.05 | 12.84 | 3.81 |
| A/CNK | 0.56 | 0.95 | 1.06 | 0.84 | 1 | 1.37 | 0.99 | 1.42 | 0.43 | 1.21 | 1.13 | 1.08 | 1.42 | 0.43 |
| A/NK | 0.92 | 1 | 1.1 | 0.86 | 1.01 | 1.42 | 1.07 | 1.49 | 0.95 | 1.27 | 1.24 | 1.18 | 1.49 | 0.86 |
| Alt.Index | 66.49 | 79.98 | 88.39 | 92.40 | 91.71 | 83.94 | 87.10 | 86.05 | 49.88 | 85.54 | 83.77 | 86.67 | 92.40 | 49.88 |
| CCPI Index | 7.03 | 21.49 | 27.31 | 17.42 | 13.48 | 13.12 | 40.43 | 49.66 | 3.84 | 30.05 | 29.78 | 24.47 | 49.66 | 3.84 |
| Total alkali | 10.72 | 7.6 | 9.66 | 10.1 | 11.49 | 10.13 | 7.78 | 7.39 | 9.52 | 8.73 | 8.44 | 8.18 | 11.49 | 7.39 |
| FI | 71.23 | 96.94 | 97.48 | 98.63 | 99.14 | 94.41 | 97.74 | 96.35 | 56.26 | 97.11 | 98.25 | 98.20 | 99.14 | 56.26 |

* MC9 to MC12 are non-radioactive samples. Alt Index: Alteration Index = $100*(MgO+K_2O)/(MgO+K_2O+CaO+Na_2O$;
CCPI: Chlorite Carbonate Pyrite Index = $100*(MgO+FeO)/(MgO+FeO+K_2O+Na_2O)$. FI: Felsic Index= $100*(Na_2O+K_2O)/(Na_2O+K_2O+CaO)$

## DISCUSSION

Many ore deposits are associated with calderas, especially with ring fracture volcanism similar to the Canyon Rhyolite (Heald and Hayba, 1987). Studies of many volcanic systems in the western United States (Zielinski, 1978; Zielinski, 1985; Castor and Henry, 2000) show an association of high U and Th concentrations with silicic volcanic rocks, generally classified as "rhyolite". Global studies (Cuney and Kyser, 2009) point to high uranium concentrations in peralkaline volcanic rocks, but high values are also found in alkali rhyolites, metaluminous rhyolites, and some calc-alkaline tuffs (Castor and Henry, 2000). The Mohar uranium mineralization confined to peralkaline to peraluminous rhyolite, is restricted to a small area, and is within the rhyolite mesa structure (or caldera), which, presents a geologic setting, where, hydrothermal activity is common during caldera-related volcanism. The small area of mineralization suggests a localized process. The study of borehole data indicates the presence of a flat body of rhyolite of varying thickness beneath the Dhala sedimentary rocks.

The data accrued suggest that the fractures and weak planes have played an important role in the area for the uranium mineralization. Core studies of mineralized boreholes have indicated fractures as the loci of mineralization, as the radioactivity is chiefly confined to such fractures. The alteration mineral assemblages typical of hydrothermal activity are noticed. Petrological studies bring out evidences of hydrothermal activity affecting and altering the host rhyolite along post-consolidation fractures, in the form of secondary silicification, chloritisation, carbonatisation, kaolinisation and sulfide formation. It also shows that the uranium mineralization is invariably associated with chlorite, clay, silica, pyrite, chalcopyrite (± galena and sphalerite). The presence of sulfides and chlorite imply a reducing environment prevailing at the time of formation of the uranium minerals.

The radioactivity is mainly due to coffinite with contribution from U-Ti complex, uranium adsorbed in clay and labile uranium along fracture. The occurrence of fluorite is noted in association with quartz. Geochemical data indicate a high $K_2O$ / $Na_2O$ ratio upto 12.84, possibly due to alteration. The rhyolite is mostly peralkaline to peraluminous. The felsic index is upto 99.14. The high alteration index upto 92.40 reflects a high intensity of

hydrothermal alteration. The chlorite-carbonate-pyrite index (CCPI) is moderately high in a few samples. The trace element contents indicate higher value of Cu and Co for the radioactive samples as compared to the non- radioactive samples implying the enrichment of these elements with uranium in hydrothermal solutions.

The rhyolite-hosted uranium occurrence in Mohar is probably formed by more than one geological process. Uranium from the basement Bundhelkhand Granite (av.5.7 ppm, Bhattacharya et.al 2006) or rhyolite (average 30 ppm) provenance may have been remobilised and transported by shallow heated ground water in the $U^{+6}$ state. Uranium in acidic rocks is first converted from the primary phase to oxide coatings during vapour phase alteration (Leroy et al. 1987) making it accessible to passing of hydrothermal or supergene fluids. The presence of younger mafic suite of rocks, in the area indicates a later mafic episode, which, could have provided the thermal gradient for heating up large volumes of ground water for efficient leaching and remobilization of uranium and its deposition along structural planes of weakness on reduction. The presence of associated alteration minerals also implies that secondary processes were at work. Fluorite noted in association with quartz endorses the role of hydrothermal fluid. The concentration of this remobilised uranium occurred along fractures in the host rhyolite/tuff later in the presence of reductants, in association with sulfide and chlorite. The nature of the dominant uranium mineral (coffinite, a low temperature mineral), its association with other alteration minerals and the mode of occurrence are indicators of low temperature epigenetic mineralization due to the activity of solutions rich in Si, Ti, U, Cu and Pb. Uranium adsorbed in clay and labile uranium along fractures may indicate later episodes of limited remobilisation**.** Based on the geologic setting, mineralogy and trace element geochemistry, an epigenetic hydrothermal origin is envisaged for the Mohar uranium occurrences.

## CONCLUSION

Rhyolite-hosted uranium mineralization and the presence of high background uranium concentration in the rhyolite at Mohar is an important exploration guide. The descriptive and genetic work on volcanogenic uranium deposits is not covered extensively. The required research and field studies are challenges for us. We are optimistic that large deposits can be found in settings where large-volume fluid flow has occurred in suitable structural traps, aided by thermal or gravitational drive in the presence of reductants. The post-magmatic hydrothermal solution, mafic intrusion activity, the presence of depositional traps and reductants are the factors that facilitated uranium mineralization in the rhyolite at Mohar. Thus, we suggest that the Mohar uranium mineralization is structurally controlled, epigenetic hydrothermal-type that developed in response to a localized heat flux associated with mafic intrusive activity**.**

*Acknowledgements:* Analytical support from the physics and Chemistry Laboratories, Northern Region, is acknowledged with thanks. Thanks are due to Shri R.C. Rana for his support in map preparation and digitization.

## References

Basu, A.K. (1986) Geology of parts of Bundhelkhand Granite massif, Central India: Rec. Geol. Surv. India, v. 17(2), pp.61-124.

Bhattacharya, D. and Rao, M.K. (2006) Lithogeochemical sampling and lithostructural mapping of Mohar Cauldron, Shivpuri district, M.P. Unpublished Annual Report of Field Season 2005-2006. Atomic Minerals Directorate for Exploration and Research, Northern Region, New Delhi.

Castor, B.S. and Henry, D.C. (2000) Geology, geochemistry, and origin of volcanic rock-hosted uranium deposits in northwestern Nevada and southeastern Oregon, USA. Ore Geology Rev., v.16, pp.1-40

Cuney, M. and Kyser, K. (2009) Recent and not-so-recent developments in uranium deposits and implications for exploration. Mineral. Assoc. Canada, Short Course Series, v.39, pp.257.

Heald P., Foley, N.K. and Hayba, D.O. (1987) Comparative anatomy of volcanic- hosted epithermal deposits. Acid –sulfate and adularia-sericite types. Econ. Geol., v.82, pp. 1-26

Jain, S.C, Gaur, V.P, Shrivastava, S.K., Nambiar, K.V. and Saxena, H.P. (2001) Recent find of a cauldron structure in Bundhelkhand Craton. Geol. Surv. India, Spec. Publ., No.64, pp.289-297.

Leroy, J.L., Aniel, B. and Poty, B. (1987) The Sierra Pena Blanca (Mexico) and Meseta Los Frailles (Bolivia) — The uranium concentration mechanisms in volcanic environment during hydrothermal processes: Uranium, v.3, pp.211-234.

Nash, J. Thomas (2010) Volcanogenic uranium deposits — Geology, geochemical processes, and criteria for resource assessment: USGSy Open-File Report 2010-1001, pp.1- 99.

Pati, J.K. and Reimold, W.U. (2007) Impact cratering-fundamental progresss in geosciences and planetary science. Jour. Earth System Sci., v.116 (2), pp.81-98.

Pati J.K., Reimold, W.U. Koeberi, C., Singh, H.K. and Pati, P. (2008) DHALA- A New, Complex, Paleoproterozoic Impact

Structure in Central India. Large Meteorite Impacts and Planetary Evolution IV, pp. 3041.

RAHMAN, A. and ZAINUDDIN, S.M. (1993) Bundhelkhand Granites: an example of collision related Precambrian magmatism and its relevance to the evolution to the Central Indian Shield. Jour. Geol., v.101, pp.413-419.

ROSS R. LARGE, BRUCE GEMMELL, J., HOLGER PAULICK and DAVID L. HUSTON (2001) The Alteration Box Plot: A Simple Approach to Understanding the Relationship between Alteration Mineralogy and Lithogeochemistry Associated with VHMS Deposits. Econ. Geol., v.96, pp. 1-14,

SHARMA, K.K. and RAHMAN, A. (1998) Geological evolution and crustal growth of the Bundhelkhand craton and its relict in the surrounding regions, northern India shield. *In:* B.S. Paliwal (Ed.), The Indian Precambrian. Scientific Publishers, Jodhpur, pp.33- 43.

Zielinski, R.A. (1978) Uranium abundances and distribution in associated glassy and crystalline rhyolites of the western United States. Geol. Soc. Amer. Bull., v. 89, pp.409-414.

ZIELINSKI, R.A. (1985) Volcanic rocks as sources of uranium, *in* Uranium in Volcanic Rocks: Vienna, International Atomic Energy Agency, Tecpub-690, pp.83-95.

*(Received: 15 October 2012; Revised form accepted: 15 November 2012)*